Application of the CACM and MPMPO modules using the CMAQ model for the eastern United States

Jianjun Chen,[1] Huiting Mao,[1] Robert W. Talbot,[1] and Robert J. Griffin[1,2]

Received 31 May 2006; revised 24 July 2006; accepted 11 August 2006; published 21 October 2006.

[1] The Caltech Atmospheric Chemistry Mechanism (CACM) and the Model to Predict the Multiphase Partitioning of Organics (MPMPO) have been updated with a detailed treatment of the oxidation mechanisms and secondary organic aerosol (SOA) formation potentials of α-pinene, β-pinene, and d-limonene. The updated CACM and MPMPO modules have been incorporated into the Community Multiscale Air Quality (CMAQ) model. The revised CMAQ model was used to simulate air quality over the eastern United States, with a particular focus on New England (NE) for the period 3–4 August 2004, which was part of the International Consortium for Atmospheric Research on Transport and Transformation (ICARTT) campaign. On 3 August, 24-hour-average organic aerosol (OA) and $PM_{2.5}$ concentrations were approximately 7.0 μg m^{-3} and 13.0 μg m^{-3}, respectively, at Thompson Farm (TF), a rural site in southeastern New Hampshire. The model results (e.g., ozone (O_3), $PM_{2.5}$, and individual $PM_{2.5}$ chemical components) were compared against various observational data sets (e.g., AIRMAP, IMPROVE, SEARCH, and AIRNOW), as well as CMAQ model predictions using the CB-IV gas-phase mechanism and the SORGAM SOA module. Both CMAQ model simulations with CACM/MPMPO and with CB-IV/SORGAM predicted O_3, $PM_{2.5}$, sulfate, and ammonium reasonably well but underestimated elemental and organic carbon aerosol. SOA predictions from CACM/MPMPO and from CB-IV/SORGAM were very close for the sites where OA concentrations were available on 4 August, though sensitivity of SOA predictions at TF to domain-wide NO_x emissions and temperature variations differed significantly. Additionally, on the basis of the predicted chemical composition of OA from CMAQ with CACM/MPMPO, 24-hour averages of the ratio of the organic mass to organic carbon were determined to be in the range of 1.1 to 1.9, depending on the relative abundance of SOA and primary organics.

Citation: Chen, J., H. Mao, R. W. Talbot, and R. J. Griffin (2006), Application of the CACM and MPMPO modules using the CMAQ model for the eastern United States, *J. Geophys. Res.*, *111*, D23S25, doi:10.1029/2006JD007603.

1. Introduction

[2] Organic mass (OM) is an important component of atmospheric aerosols, generally accounting for 30–60% of fine particle mass [*Chow et al.*, 1994; *Tanner et al.*, 2004]. A substantial fraction of OM is secondary organic aerosol (SOA), which is formed in the atmosphere from the gas-to-particle partitioning of the oxidation products of gas-phase hydrocarbons. Examples of SOA formation mechanisms include absorption into existing aerosol-phase organics [*Pankow*, 1994], dissolution into aerosol-phase water [*Saxena and Hildemann*, 1996; *Aumont et al.*, 2000], heterogeneous or particle-phase reactions [*Jang et al.*, 2002; *Kalberer et al.*, 2004], and cloud-phase reactions [*Ervens et al.*, 2004; *Lim et al.*, 2005].

[3] Because of the complexity of SOA formation processes, treatment of SOA formation is a major source of uncertainty in three-dimensional particulate matter (PM) models [*Seigneur*, 2001; *Pun et al.*, 2003]. Typical three-dimensional air quality models use empirical approaches based on environmental chamber data to simulate SOA formation [*Schell et al.*, 2001; *Pun et al.*, 2003]. Recently, mechanistic or semimechanistic approaches for modeling SOA have emerged in the literature and are considered to be the future direction of more realistic SOA modeling [*Griffin et al.*, 2005; *Kanakidou et al.*, 2005; *Johnson et al.*, 2006].

[4] An example of such a mechanistic approach that has been used in three-dimensional air quality models is the Caltech Atmospheric Chemistry Mechanism (CACM) and the Model to Predict the Multiphase Partitioning of Organics (MPMPO) [*Griffin et al.*, 2002a, 2002b, 2003; *Pun et al.*, 2002]. CACM predicts the products of gas-phase oxidation of volatile organic compounds (VOCs), and MPMPO simulates the phase partitioning of those that are semivolatile or nonvolatile. The CACM and MPMPO were incorporated originally into the California Institute of Tech-

[1]Institute for the Study of Earth, Oceans, and Space, University of New Hampshire, Durham, New Hampshire, USA.
[2]Also at Department of Earth Sciences, University of New Hampshire, Durham, New Hampshire, USA.

Copyright 2006 by the American Geophysical Union.
0148-0227/06/2006JD007603

nology urban-scale air quality model and applied to the South Coast Air Basin (SoCAB) of California [*Griffin et al.*, 2002b, 2003]. *Griffin et al.* [2005] updated the CACM and MPMPO to mimic SOA yields from laboratory chambers. *Chen and Griffin* [2005] further updated the CACM mechanism with a detailed treatment of chemistry for α-pinene, β-pinene, and d-limonene.

[5] In this study, the CACM and MPMPO with the updates of *Griffin et al.* [2005] and *Chen and Griffin* [2005] have been incorporated into a state-of-the-science regional air quality model, the Community Multiscale Air Quality (CMAQ) model [*Byun and Ching*, 1999], and have been applied over the eastern United States. Focus is placed on the New England (NE) region, which is heavily influenced by biogenic hydrocarbons [*Lamb et al.*, 1993]. The objectives of the study are: to evaluate the performance of the updated CACM/MPMPO in simulating ambient SOA formation; to compare the updated CACM/MPMPO with default gas-phase chemistry and SOA modules in the CMAQ model; to evaluate the sensitivity of the different SOA modules to variations in temperature and emissions of oxides of nitrogen (NO_x) and VOCs; to quantify aqueous-phase SOA concentrations relative to the total in the MPMPO module; and to investigate the OM to organic carbon (OC) ratio predicted by the MPMPO module. For the first of these objectives, CACM/MPMPO output will be compared to high-time-resolution aerosol mass spectrometer (AMS) data for the first time.

2. Models and Measurement Data

2.1. CACM and MPMPO

[6] CACM is designed to characterize the formation of O_3 and products that could potentially contribute to SOA from the oxidation of VOCs [*Griffin et al.*, 2002a]. CACM lumps parent VOCs into categories based on their SOA formation potentials, reactivity, and structure. Examples of such lumped species are aromatic low and aromatic high, where low and high represent relative SOA formation potentials. CACM is an intermediate approach between the nonspecific SAPRC mechanism [*Carter*, 1990] and the fully explicit Master Chemical Mechanism (MCM) [*Jenkin et al.*, 2003; *Saunders et al.*, 2003]. It allows for an increased level of detail while still maintaining reasonable computational demands.

[7] The MPMPO calculates the partitioning of CACM-predicted semivolatile oxidation products between the gas and aerosol phases using ten surrogate species [*Griffin et al.*, 2003]. Two processes that are responsible for SOA formation are treated simultaneously, in contrast to only one process that is typically treated in other SOA modules. The first is absorption into existing aerosol OM (i.e., primary organic aerosol, POA, or preexisting SOA). This is characterized by an absorption coefficient, $K_{om,i}$ (m^3 μg^{-1}) [*Pankow*, 1994]:

$$K_{om,i} = \frac{O_i}{G_i M_o} = \frac{RT}{MW_{om} 10^6 \gamma_i p^o_{L,i}} \quad (1)$$

where O_i ($\mu g\ m^{-3}$) and G_i ($\mu g\ m^{-3}$) are the organic aerosol- and gas-phase concentrations of compound i, respectively, M_o ($\mu g\ m^{-3}$) is the total aerosol-phase OM concentration (including POA, if present), R is the ideal gas constant (8.206×10^{-5} m^3 atm mol^{-1} K^{-1}), T is temperature (K), MW_{om} is the average molecular weight of the organic phase (g mol^{-1}), γ_i is the activity coefficient of compound i, and $p^o_{L,i}$ is the subcooled liquid vapor pressure (atm) of compound i at temperature T.

[8] The second process is dissolution into aerosol-phase water, which is represented by Henry's Law:

$$A_i = \frac{G_i(\mathrm{LWC})HL_i}{\gamma_{aq,i}} \quad (2)$$

where A_i is the aqueous aerosol-phase concentration of species i ($\mu g\ m^{-3}$), HL_i is its Henry's Law coefficient (($\mu g\ \mu g^{-1}\ H_2O$)/($\mu g\ m^{-3}$ air)), LWC is the aerosol liquid water content ($\mu g\ H_2O\ m^{-3}$ air), and $\gamma_{aq,i}$ is the activity coefficient of species i in the aqueous aerosol phase, normalized by that at infinite dilution. Further dissolution of the oxidation products into organic ions is also considered.

[9] *Chen and Griffin* [2005] updated the CACM with detailed oxidation mechanisms for α-pinene, β-pinene, and d-limonene and used an absorption module based on *Pankow* [1994] to simulate SOA formation from oxidation of these three compounds in laboratory experiments. For application in three dimensions, over forty simulated oxidation products for α-pinene, β-pinene, and d-limonene are lumped into the three original biogenic surrogate species in the MPMPO module plus a newly created surrogate species (2,10-dinitrato-pinane).

[10] To improve the model performance for the experiments with low initial VOC concentrations in the simulations of *Chen and Griffin* [2005], a mechanism involving dimer formation of di- and multifunctional acid species proposed by *Jenkin* [2004] has also been adopted. This is represented by inclusion of a pseudo-unimolecular reaction

$$\mathrm{acid(gas)} \rightarrow \mathrm{acid(aerosol)} \quad (3)$$

for each of the 15 multifunctional acid species generated from oxidation of the monoterpenes. The reaction was assigned a rate coefficient $k = k'\Sigma[\mathrm{acid(gas)}]$ [*Jenkin*, 2004], where $\Sigma[\mathrm{acid(gas)}]$ is the sum of the gas-phase concentrations of all multifunctional acids generated from α-pinene, β-pinene, and d-limonene and $k' = 1.5e{-}35 \times \exp(14770/T)$ cm^3 $molecule^{-1}$ s^{-1}, a value decreased by three orders of magnitude compared to that used in *Jenkin* [2004], in order to fit experimental data. Reaction (3) is treated as a gas-phase reaction in CACM, leading to an assumed nonvolatile dimer [*Jenkin*, 2004]. The mass of the dimer is added to the SOA mass, with the corresponding monomer acid mass no longer available for partitioning using MPMPO.

[11] Simulations based on the four MPMPO surrogate species with the additional acid gas-to-particle transfer process were evaluated using the photooxidation experimental data from *Hoffmann et al.* [1997] and *Griffin et al.* [1999]. Figure 1 shows the comparison of observed and predicted final SOA for these experiments. Reasonable agreement is achieved, indicating that use of the four surrogate species is appropriate. After the update, five individual monoterpene species (i.e., α-pinene, β-pinene, d-limonene, α-terpineol, and γ-terpinene) and their products

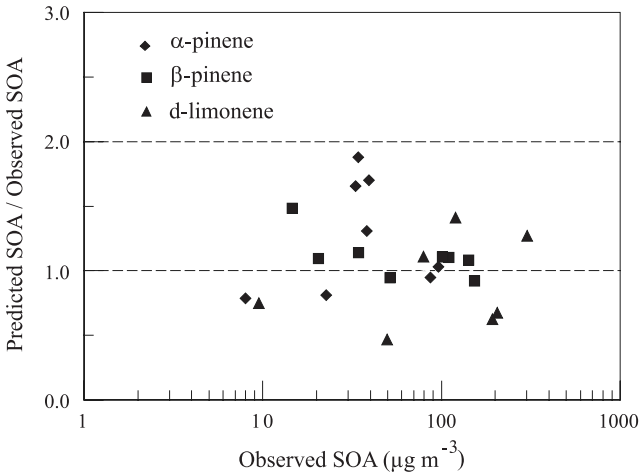

Figure 1. Comparison of observed SOA during photo-oxidation experiments with those predicted by CACM and an absorption module based on four surrogate species (observed data from *Hoffmann et al.* [1997] and *Griffin et al.* [1999]).

are now treated explicitly in CACM and accounted for in the surrogates used in MPMPO.

[12] Within CMAQ, CACM was coupled to a general Rosenbrock ordinary differential equation solver [*Sandu et al.*, 1997]. Existing gas-phase chemistry mechanisms in CMAQ include CB-IV [*Gery et al.*, 1989], RADM [*Stockwell et al.*, 1990], and SAPRC99. In CMAQ, inorganic aerosol formation is simulated with ISORROPIA [*Nenes et al.*, 1998], and organic aerosols are simulated using SORGAM [*Schell et al.*, 2001]. Because MPMPO interacts with the inorganic aerosol module in order to treat the effects of additional water uptake by SOA and dissociated SOA ions on the inorganic partitioning, the ISORROPIA module from the MADRID model that has that capability [*Zhang et al.*, 2004a] was used in this study.

2.2. Measurement Data

[13] Measurement data were taken from a wide range of sources. Hourly O_3, 24-hour average PM with diameters less than 2.5 micron ($PM_{2.5}$), and 24-hour average speciated $PM_{2.5}$ were taken from a variety of programs, including the Atmospheric Investigation, Regional Modeling, and Prediction (AIRMAP) program [*Talbot et al.*, 2005], EPA Air Quality System (AQS), the Southeastern Aerosol Research Characterization Study (SEARCH) [*Hansen et al.*, 2003], and the Interagency Monitoring of Protected Visual Environments (IMPROVE) [*Malm et al.*, 1994]. Highly time-resolved chemical mass concentrations for speciated $PM_{2.5}$ were drawn from an Aerodyne AMS [*Jayne et al.*, 2000] deployed at the Thompson Farm (TF), a rural site in southeastern New Hampshire, as part of International Consortium for Atmospheric Research on Transport and Transformation (ICARTT). The TF site is part of the AIRMAP network of atmospheric observatories operated by the University of New Hampshire [*Talbot et al.*, 2005]. Additionally, observed PM from a particle-into-liquid sampler (PILS) measurement [*Sullivan et al.*, 2004] on board the NOAA P3 aircraft was used to evaluate vertical predictions of PM.

3. Model Applications

[14] The CMAQ model implemented with CACM/MPMPO was used to simulate air quality for the eastern United States. While an earlier version of CACM was applied to a similar spatial domain previously using CMAQ [*Pun et al.*, 2003], this is the first application of the full MPMPO and the updated CACM [*Chen and Griffin*, 2005; *Griffin et al.*, 2005] within this framework. For comparison purposes, simulations were also performed using the default CB-IV/SORGAM modules. The model domain is shown in Figure 2. It has a 62 × 66 horizontal grid with a resolution of 36 km. Vertically, 21 layers are specified with a σ-pressure coordinate extending from the surface to 10,000 Pa.

[15] The MPMPO module uses the UNIFAC method to calculate activity coefficients for the surrogate species in the aerosol organic and aqueous phases [*Fredenslund et al.*, 1977], which dramatically increases the computational time. It was found to be computationally too intensive to simulate the entire modeling domain while including the UNIFAC calculation. Therefore the smaller domain shown in Figure 2 was selected to evaluate whether assuming unity for all activity coefficients yields results similar to those from the full UNIFAC calculation. In order to focus on those areas where SOA formation was most significant, only those cells in which predicted SOA concentrations were greater than 0.5 μg m^{-3} were considered in this analysis. Simulation within this small domain for these cells shows that SOA predictions while assuming unity for activity coefficients were within ±5% of the base predictions. This is largely due

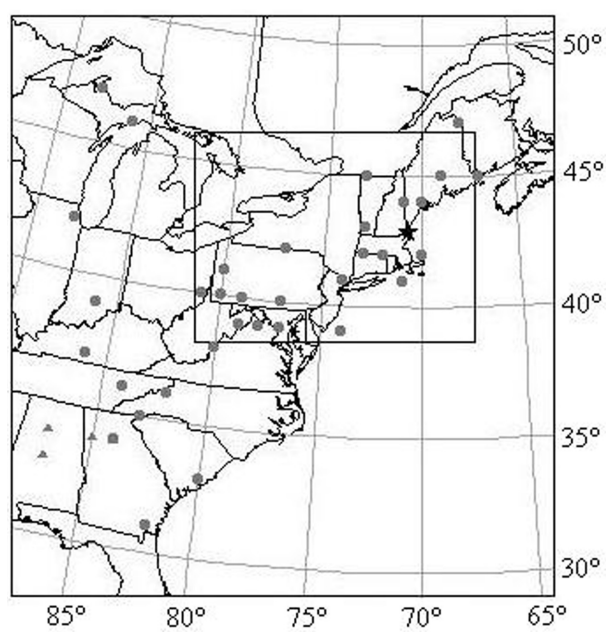

Figure 2. Modeling domain for this study. The small domain was used for a sensitivity analysis with activity coefficient calculation on or off. AIRMAP sites are stars, SEARCH sites are triangles, and IMPROVE sites are circles.

to the fact that the majority of simulated SOA formation results from biogenic sources. Therefore activity coefficients do not deviate significantly from unity because of the molecular similarity of the species. Thus, when the MPMPO-incorporated CMAQ model was applied to the entire modeling domain, the activity coefficients of all organic species in the condensed phases were assumed to be one.

[16] The episode of 3–4 August 2004 (UTC) is chosen for simulation, as 3 August experienced one of the highest OM concentrations measured during ICARTT using filters at TF (L. D. Ziemba et al., Aerosol acidity in northern New England: Temporal trends and source region analysis, submitted to *Journal of Geophysical Research,* 2006). Much of NE featured clear or partly cloudy skies with high temperatures in the range of 27 to 32°C during the daytime of 3 August 2004. A cold front pushed through NE during 4 August 2004. Twenty-four-hour average OM and $PM_{2.5}$ concentrations were approximately 7.0 μg m^{-3} and 13.0 μg m^{-3}, respectively, at TF on 3 August. The maximum 1-hour O_3 mixing ratio during 3 August 2004 reached 95 parts per billion (ppb) at Appledore Island (AI), which is one of the Isles of Shoals in the Gulf of Maine and is host to another AIRMAP observatory.

[17] Emission profiles have been processed with the Sparse Matrix Operator Kernel Emissions (SMOKE1.0) system, as in the work by *Mao et al.* [2006]. Anthropogenic emissions are based on the U.S. National Emissions Inventory 99 Version 2, while biogenic emissions are calculated with the Biogenic Emissions Inventory System (BEIS3.09) model. Because the VOCs emissions data processed by SMOKE were formatted for the CB-IV mechanism, they had to be transformed for use with CACM. This was done using the VOC speciation profile for the SoCAB, as was done by *Pun et al.* [2003]. The monoterpene speciation was based on annual emission estimates for individual monoterpenes for North America from *Guenther et al.* [2000]. Meteorological fields were simulated with the PSU/NCAR Mesoscale Modeling System Generation 5 version 3.4 (MM5). Additional details of model setup and configuration also are given by *Mao et al.* [2006].

4. Model Results

[18] In this study, model results are compared with measured values for O_3, $PM_{2.5}$, and $PM_{2.5}$ composition at various surface locations. Vertical profiles are also considered. Only species with lifetimes in excess of a few hours are shown because of the spatial resolution of the host model.

4.1. O_3 Predictions

[19] Figure 3 shows the simulated and observed hourly average O_3 mixing ratios at the surface at TF and AI. Simulations with both CACM and CB-IV generally are able to capture the temporal variations of O_3 mixing ratios at AI, but not at TF. For 3 August, 2004, at TF, CACM accurately predicts the O_3 peak, while CB-IV underpredicts the O_3 peak by 11%. For the same day at AI, CACM and CB-IV overpredict the O_3 peak by 36% and 23%, respectively. The only difference between the simulations is the gas-phase chemical mechanism used. Disparities in their

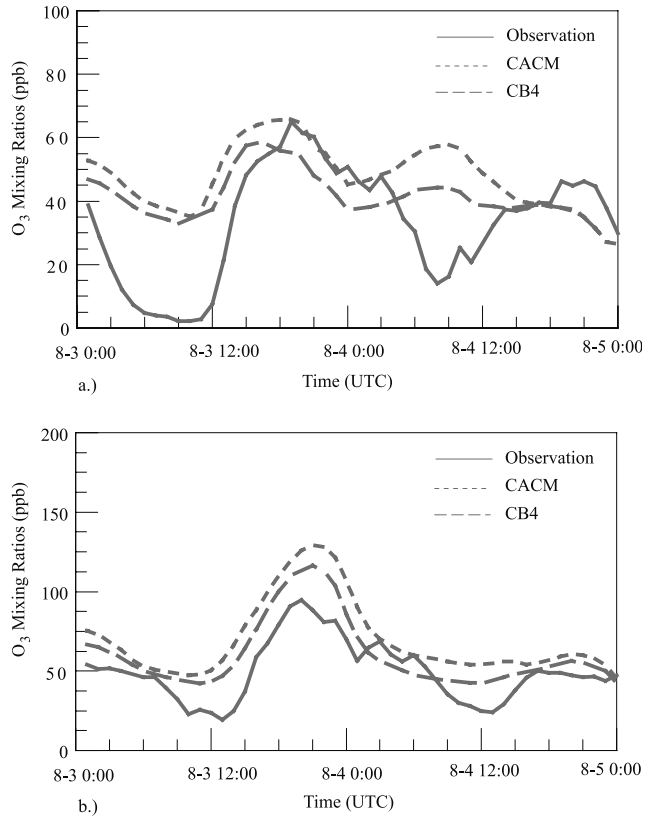

Figure 3. Measured and modeled O_3 mixing ratios: (a) TF and (b) AI.

VOC aggregation scheme, reaction rate constants, product yields, etc. likely lead to the discrepancies in modeled O_3 mixing ratios.

[20] An interesting feature in the O_3 profiles at TF is the depletion of O_3 at night, which occurs frequently at this site [*Talbot et al.*, 2005]. This was not captured by the model. This is potentially caused by use of a minimum vertical diffusion coefficient, K_{zz}, of 1.0 m^2/s. If the minimum K_{zz} is assigned to be 0.1 m^2/s [*Zhang et al.*, 2004b], the O_3 predictions at night from the CB-IV mechanism could be decreased to 20 ppb, still significantly higher than observed values. The model probably underestimates dry deposition losses, which were found to be responsible for nighttime O_3 depletion at this site [*Talbot et al.*, 2005].

[21] The modeled 1-hour average O_3 mixing ratios for 3–4 August 2004 (EST) are compared to observations for approximately 400 EPA AQS sites across the modeling domain. Table 1 summarizes the model performance statistics for the CACM and CB-IV applications for 1-hour average O_3 mixing ratios when the observed O_3 mixing ratios exceed 60 ppb [*Zhang et al.*, 2004b]. The model performance in terms of mean normalized gross error (MNGE) and mean normalized bias (MNB) for both CACM and CB-IV is comparable to those reported in other studies [*Zhang et al.*, 2004b].

4.2. $PM_{2.5}$ Predictions

[22] Model-simulated, 24-hour average $PM_{2.5}$ concentrations are evaluated against measurements at 117 EPA AQS

Table 1. Performance Summary for 1-Hour Average O_3 Mixing Ratios on 3–4 August 3 2004 for CACM and CB-IV[a]

			Mean Prediction, ppb		MNGE		MNB	
Date (EST)	Data Points	Mean Observation, ppb	CACM	CB-IV	CACM	CB-IV	CACM	CB-IV
3 Aug 2004	1870	69.7	70.0	58.6	0.21	0.22	0.01	−0.16
4 Aug 2004	929	69.7	75.8	60.7	0.23	0.18	0.09	−0.12

[a]Data are from EPA AQS. MNGE, mean normalized gross error; MNB, mean normalized bias.

sites across the modeling domain. The model performance statistics are summarized in Table 2 for CACM/MPMPO and CB-IV/SORGAM. Model predictions from CACM/MPMPO are only slightly different than those from CB-IV/SORGAM. The differences are due solely to differences in the gas-phase chemical mechanism and the SOA module. The gas-phase chemical mechanism affects inorganic aerosol formation by providing gas-phase concentration fields (e.g., hydroxyl radical (OH), hydrogen peroxide (H_2O_2), and O_3). Predictions of the concentrations of primary species (e.g., elemental carbon (EC), POA, and other $PM_{2.5}$ species) are independent of the gas-phase chemical mechanism and SOA modules. For both CACM/MPMPO and CB-IV/SORGAM for 24-hour average $PM_{2.5}$, the MNGE and MNB are approximately 38% and −24%, respectively, which are values comparable to other studies [*Zhang et al.*, 2004b].

[23] Model-predicted, 24-hour average compositions are also compared to speciation measurements from the AIRMAP, SEARCH, and IMPROVE programs. A summary of model performance statistics is given in Table 3. Among the 45 data pairs, 43 data points are for 4 August 2004 (EST) because the SEARCH and IMPROVE programs did not sample on 3 August 2004. The remaining two pairs are from TF from AIRMAP and Jefferson Street, Atlanta, Georgia, from SEARCH on 3 August 2004. For these sites, the performance of total $PM_{2.5}$ mass predictions is consistent with that for the EPA AQS sites given in Table 2. Model simulations using CACM/MPMPO and CB-IV/SORGAM show only minor differences in percentage for sulfate, nitrate, ammonium, EC, and OM predictions. For the predictions of individual chemical species, MNGE is largest for nitrate and smallest for ammonium. On the basis of MNE, both OM and EC are underestimated significantly. The underprediction of EC may reflect underestimation of EC emissions because EC is purely a primary, nonreactive species in the model. OM, however, consists of both primary and secondary material. The slight difference in terms of OM predictions reflects the difference in SOA predictions, as will be discussed subsequently.

[24] Figure 4 shows the AMS-measured and model-predicted temporal profiles for major aerosol species at TF. The AMS is able to produce highly time-resolved chemical mass concentrations for sulfate, ammonium, nitrate, and OM in aerosols with aerodynamic diameter less than approximately 1 μm. However, a study in Mexico City [*Salcedo et al.*, 2005] shows that AMS-measured species plus black carbon and soils are a good approximation for $PM_{2.5}$. For this reason, model-predicted concentrations of $PM_{2.5}$ species are compared to AMS-measured values.

[25] Model simulations with CACM/MPMPO and with CB-IV/SORGAM produce very similar temporal profiles for ammonium, nitrate, and sulfate because the same basic inorganic aerosol module is used. Besides missing one significant short-lived observed peak in both ammonium and sulfate, observed temporal profiles for ammonium and sulfate are followed adequately by the model output. The model predicts a nitrate peak that is not evident from observations.

[26] Simulations significantly underpredict the OM concentrations at this site. However, the correlations between modeled hourly OM concentrations and those measured with the AMS are 0.61 for CACM/MPMPO and 0.51 for CB-IV/SORGAM, indicating that the temporal variations of AMS-measured OM were characterized by the model to a certain extent, with slightly better performance for CACM/MPMPO. The differences in the comparisons for the high-time resolution data indicate that comparison of model output using 24-hour filter data should be done with caution. Figure 4 indicates significant differences between CACM/MPMPO and CB-IV/SORGAM despite similar predicted 24-hour average SOA concentrations.

[27] Figure 4 also shows the model predicted EC concentrations at this site compared to the measurement from an aethalometer. Modeled EC shows diurnal cycles that are not obvious from the observations. Averaged over the 48-hour period, modeled EC is actually approximately 20% higher than observed EC at this site, in contrast to the overall EC performance in the model domain, as indicated in Table 3.

[28] Model predictions of vertical profiles have been compared to observed values from a PILS measurement on board the NOAA P3 aircraft. PILS measures water-soluble aerosol species at a time resolution of 60–90 s. The

Table 2. Performance Summary for 24-Hour Average $PM_{2.5}$ Concentrations on 3–4 August 2004 for CACM/MPMPO and CB-IV/SORGAM[a]

	Mean Observation,	Mean Prediction, μg m^{-3}		MNGE		MNB	
Date (EST)	μg m^{-3}	CACM/MPMPO	CB-IV/SORGAM	CACM/MPMPO	CB-IV/SORGAM	CACM/MPMPO	CB-IV/SORGAM
3 Aug 2004	20.1	14.6	14.7	0.37	0.37	−0.23	−0.22
4 Aug 2004	21.0	15.1	15.3	0.38	0.39	−0.25	−0.24

[a]Data are from EPA AQS. MNGE, mean normalized gross error; MNB, mean normalized bias.

Table 3. Performance Summary for 24-Hour Average Concentrations of $PM_{2.5}$ and Individual $PM_{2.5}$ Species for CACM/MPMPO and CB-IV/SORGAM[a]

Species	Data Points	Mean Observation, $\mu g\ m^{-3}$	Mean Prediction, $\mu g\ m^{-3}$		MNGE		MNB	
			CACM/MPMPO	CB-IV/SORGAM	CACM/MPMPO	CB-IV/SORGAM	CACM/MPMPO	CB-IV/SORGAM
$PM_{2.5}$	45	16.70	13.70	14.10	0.33	0.36	−0.17	−0.15
Sulfate	44	7.13	7.98	8.55	0.52	0.60	0.32	0.39
Nitrate	44	0.28	0.19	0.18	1.34	1.23	−0.06	−0.03
Ammonium	15	2.73	2.74	2.71	0.14	0.15	0.03	0.02
EC	44	0.80	0.39	0.39	0.52	0.52	−0.45	−0.45
OC	44	3.82	1.26	1.18	0.66	0.69	−0.66	−0.69

[a]Data are from the SEARCH, IMPROVE, and AIRMAP programs. Ammonium concentrations for most sites from the IMPROVE program are missing. MNGE, mean normalized gross error; MNB, mean normalized bias.

position of the NOAA P3 aircraft is averaged over the PILS measurement time to yield the average position for that measurement. The average position of the aircraft is then mapped onto the modeling cells. To construct the vertical profiles, the observational points and the corresponding model predictions are averaged for every 200 m extending from the surface to an altitude of 3 km. The modeled vertical profiles for sulfate and ammonium follow the

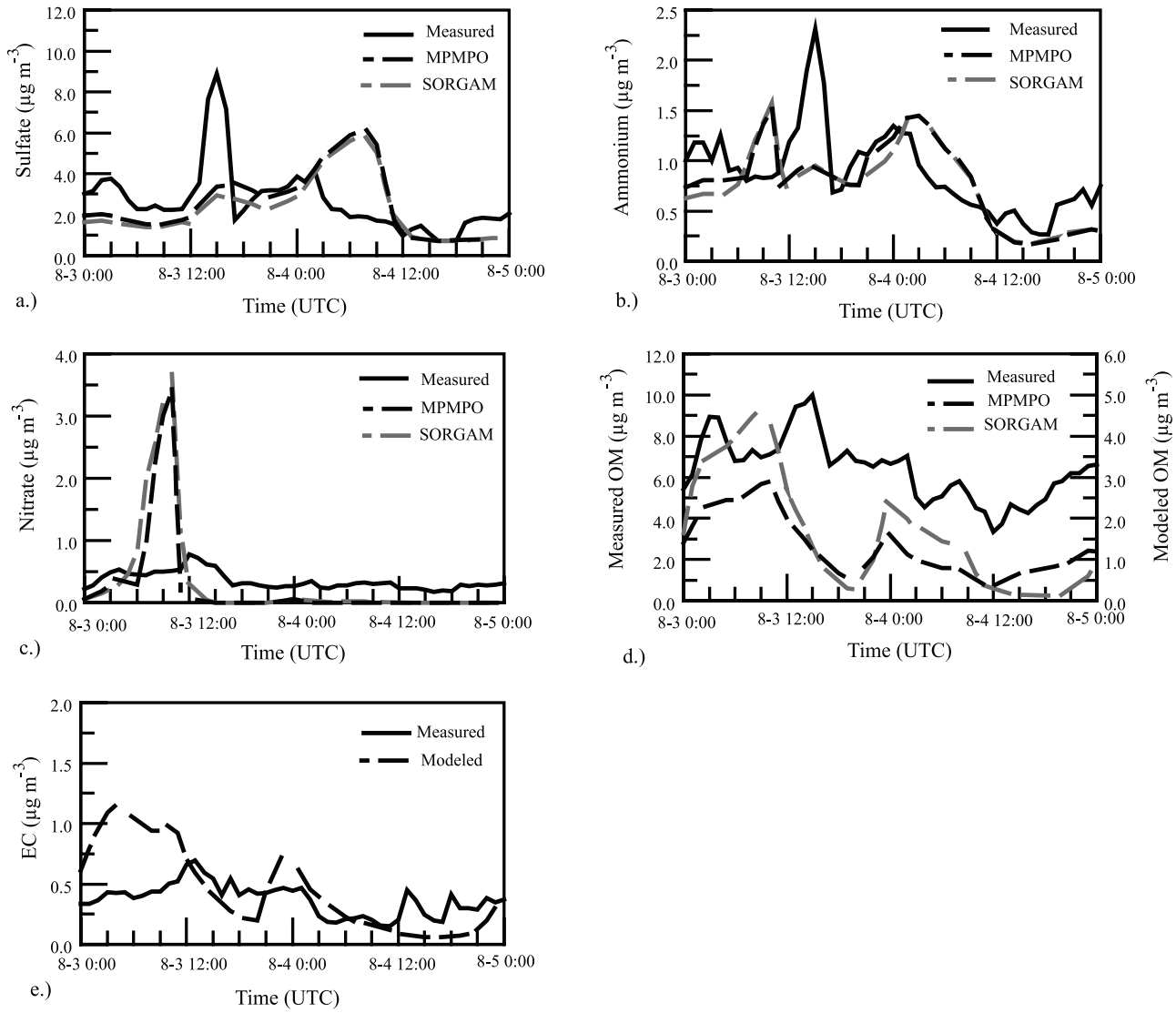

Figure 4. Comparisons of AMS_measured temporal profiles for (a) sulfate, (b) ammonium, (c) nitrate, and (d) OM and (e) aethalometer-measured EC with simulations with CACM/MPMPO and CB-IV/SORGAM at TF. Note the difference in scale between measured and modeled OM. In the case of EC, simulations with CACM/MPMPO and CB-IV/SORGAM produce the same modeled values.

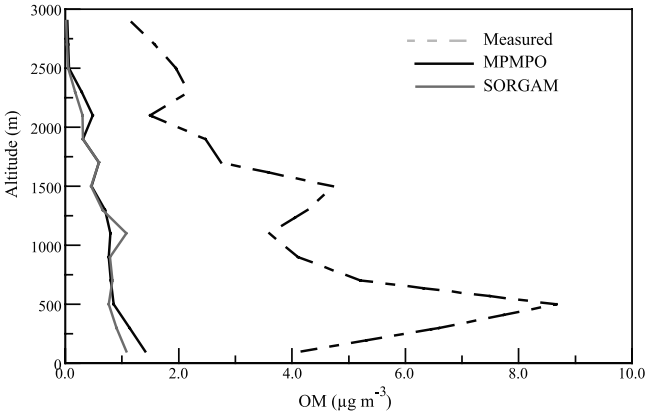

Figure 5. Comparison of observed vertical profiles for OM from a PILS measurement on board the NOAA P3 aircraft with those predicted by CACM/MPMPO and CB-IV/SORGAM.

observed ones reasonably well. Therefore only the vertical profile for OM is discussed here. Measured water-soluble OC is multiplied by 2.25 to yield approximate total OM concentrations [R.J. Weber, Georgia Institute of Technology, personal communication].

[29] Figure 5 shows the comparison between observed and model-predicted vertical profiles for OM. As with the AMS, the PILS collected particles with diameters smaller than approximately one micron; model predicted $PM_{2.5}$ OM concentrations are again shown in Figure 5. The vertical OM profile is very similar for CACM/MPMPO and CB-IV/SORGRAM. OM concentrations are significantly underestimated. The relative bias is approximately −70% at the surface and approximately −97% at the altitude of 3 km, indicating poorer model performance at greater height. *Heald et al.* [2005] found that observed OM concentrations in the free troposphere were also 10–100 times higher than model values computed using a standard two-product simulation of SOA formation based on chamber data. They suggest that a large, sustained source of SOA in the free troposphere is the oxidation of long-lived organic compounds that are not captured by current SOA modules.

4.3. SOA Predictions

[30] Figure 6 shows the predicted 24-hour average SOA on 3–4 August 2004 from CACM/MPMPO and CB-IV/SORGAM. The modeled SOA within this domain is derived mainly from monoterpenes. The spatial distributions of SOA are coincident with biogenic VOC emissions. For 3 August 2004, CB-IV/SORGAM predicts high SOA formation in the northeastern United States, particularly in Maine, as well as in places around Lake Superior. Peak 24-hour SOA concentrations occurring in Maine and Minnesota reach approximately 4.1 μg m^{-3}. For the same day, CACM/MPMPO yields high SOA predictions in the northeastern United States, New Brunswick, the southeastern United States, and places around the Great Lakes. Maximum 24-hour SOA concentrations are approximately 2.2 μg m^{-3}. For 4 August 2004, CB-IV/SORGAM produces high SOA formation in the southeastern United States, with peak values of 3.9 μg m^{-3} occurring in Georgia. CACM/MPMPO also produces strong SOA formation in the southeastern United States, with peak values of 3.6 μg m^{-3} in Georgia. The differences in predicted SOA from CACM/MPMPO and CB-IV/SORGAM mainly reflect differences in their predictions of biogenic SOA. Averaged over the entire modeling domain and throughout the modeling episode, however, SOA prediction from CACM/MPMPO is 51% higher than that from CB-IV/SORGAM. This indicates that the SOA predictions from CACM/MPMPO are spatially more spread than predictions from CB-IV/SORGAM. This is likely because CACM/MPMPO also tracks SOA formation from oxidation of the first and second generation products, while CB-IV/SORGAM assumes instantaneous SOA formation upon oxidation of parent hydrocarbons. This again underscores why use of 24-hour filter data for model comparison of simulated OM concentrations is not the most appropriate technique.

[31] CACM/MPMPO and CB-IV/SORGAM both underestimate OM concentrations at TF. One potential reason is the inaccuracy of fine POA emissions. The AMS-measured, 24-hour average OM concentration was 7.5 μg m^{-3}. Following the approach of *deGouw et al.* [2005], the ratio of the AMS signal at m/z = 44 to the total organic signal suggests that on 3 August 2004, 35–65% of OM at TF was secondary in nature (L. D. Cottrell et al., Submicron particles at Thompson Farm during ICARTT measured using aerosol mass spectrometry: Organic aerosol and relationships to estimates of photochemical age, manuscript in preparation, 2006). Assuming that 50% of OM at TF is SOA on that day, the resulting POA concentration would be 3.75 μg m^{-3}, approximately five times the modeled value of 0.77 μg m^{-3}. On the same day, the EC concentration is predicted by the model reasonably well, as shown in Figure 4. However, this does not suggest that POA should also be reasonably predicted by the model because the current emission inventory is not able to capture substantial variations of the ratio of OC to EC in emissions from various sources [*McDonald et al.*, 2000; *Shah et al.*, 2004].

[32] Although this factor of five under prediction is unlikely to be applicable to the entire modeling domain, a sensitivity analysis has been performed to investigate the response of SOA predictions if the POA concentration is increased by a factor of five. For TF, CB-IV/SORGAM yields a 24-hour average SOA prediction of 2.3 μg m^{-3} on 3 August 2004, which is 0.61 μg m^{-3}, or 37%, higher than the base-case SOA prediction. This also increases the total modeled OM concentration to 6.0 μg m^{-3}. CACM/MPMPO predicts a SOA concentration of 1.4 μg m^{-3}, an increase of 0.4 μg m^{-3}, or 43%, compared to the base case, and increases the total modeled OM to 5.2 μg m^{-3}. With the five fold increase in POA levels, SOA only increases by approximately 40%, indicating that simulated SOA formation in this scenario is limited by the availability of condensing material. With the increase of POA levels, modeled OM is still smaller than that observed, indicating that additional SOA formation is needed. Reasons for underestimation of SOA at this site may include: uncertainties associated with the gas-phase mechanism and SOA formation module (e.g., vapor pressure values used for SOA products); the underestimation of parent hydrocarbons that are responsible for SOA formation; lack of a detailed treatment of polymerization processes [*Jang et al.*, 2002; *Kalberer et al.*, 2004] and potential cloud-phase SOA

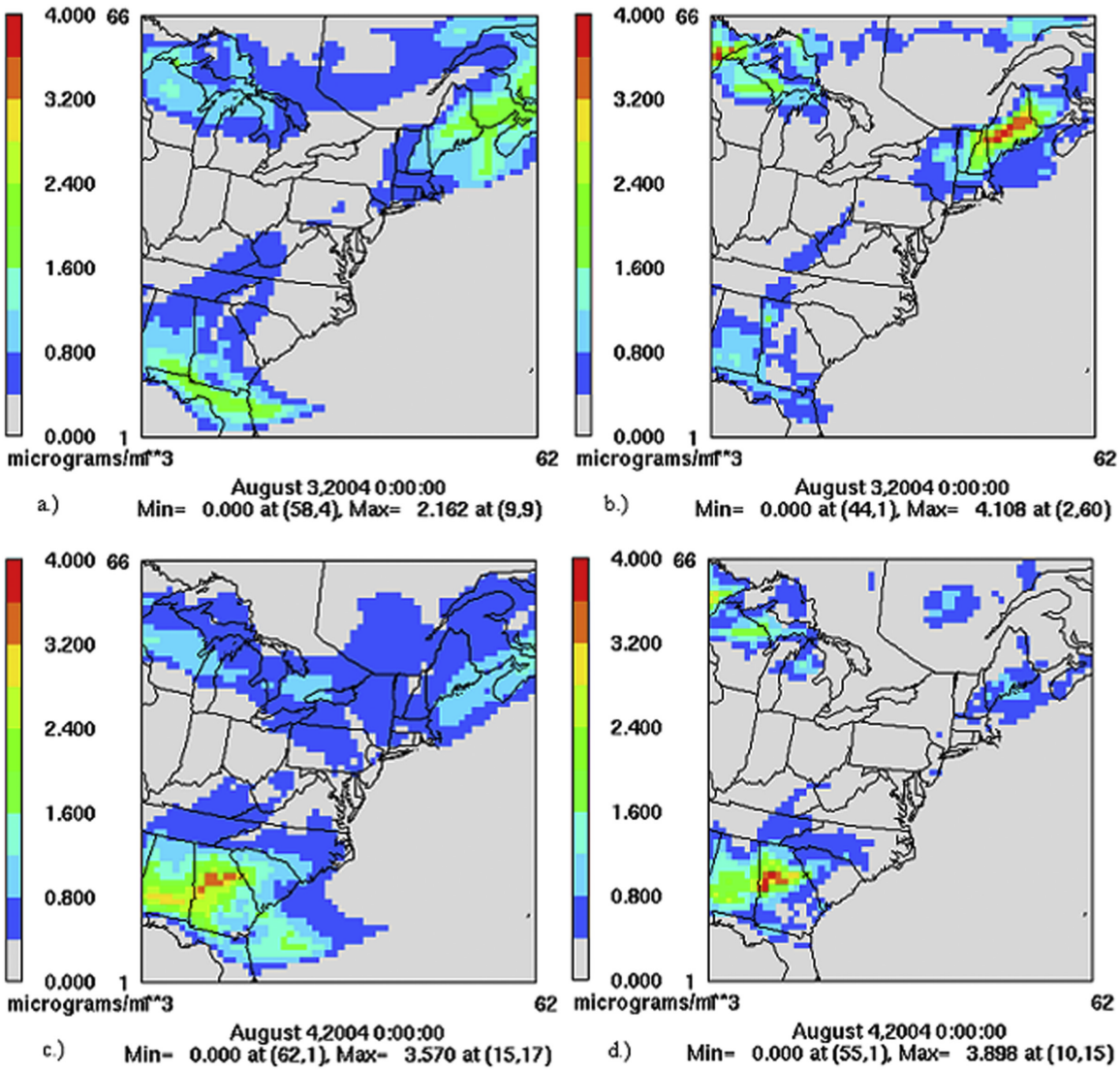

Figure 6. Predictions of 24-hour average SOA: (a) CACM/MPMPO on 3 August 2004 (UTC), (b) CB-IV/SORGAM on 3 August 2004 (UTC), (c) CACM/MPMPO on 4 August 2004 (UTC), and (d) CB-IV/SORGAM on 4 August 2004 (UTC).

formation processes [*Ervens et al.*, 2004; *Lim et al.*, 2005]; lack of consideration of SOA formation from isoprene and sesquiterpenes [*Vizuete et al.*, 2004; *Kroll et al.*, 2005a]; and lack of consideration of reactive uptake of carbonyl compounds, such as glyoxal [*Kroll et al.*, 2005b; *Hastings et al.*, 2005; *Liggio et al.*, 2005].

4.3.1. SOA Sensitivity Study

[33] The sensitivity of SOA predictions to NO_x, VOC, and temperature variations is also studied for comparison to recent experimental results and to recent modeling results for the SoCAB performed using similar techniques [*Vutukuru et al.*, 2006]. Figure 7 shows the SOA predictions at TF for 3 August 2004, for a series of sensitivity analysis studies. Twenty-four-hour average SOA prediction at TF from CACM/MPMPO is 17.2% lower when domain-wide NO_x emissions are increased by 40% from the base case compared to the case when domain-wide NO_x emissions are decreased by 40% from the base case. However, the simulation with CB-IV/SORGAM exhibits a much weaker opposite trend. TF is located in a semirural area and is probably NO_x-limited during summer [*Griffin et al.*, 2004]. NO and HO_2 compete for the reaction with organic peroxy radicals (RO_2). When NO_x increases, a smaller amount of organic acids that participate in SOA formation is formed from $RO_2 + HO_2$ reactions in the CACM mechanism, leading to less SOA formation, which is consistent with a simulation done by *Jenkin et al.* [2000] using MCM. *Presto et al.* [2005] and *Song et al.* [2005] report decreased SOA formation with increases in the NO_x to VOC ratio for α-piene and *m*-xylene, respectively, in chamber studies. The NO_x dependence of SOA formation predicted by CACM/MPMPO in the eastern United States is much stronger than that predicted by *Vutukuru et al.* [2006] for the SoCAB, probably because of the NO_x-saturated atmosphere in the SoCAB [*Kelly and Gunst*, 1990].

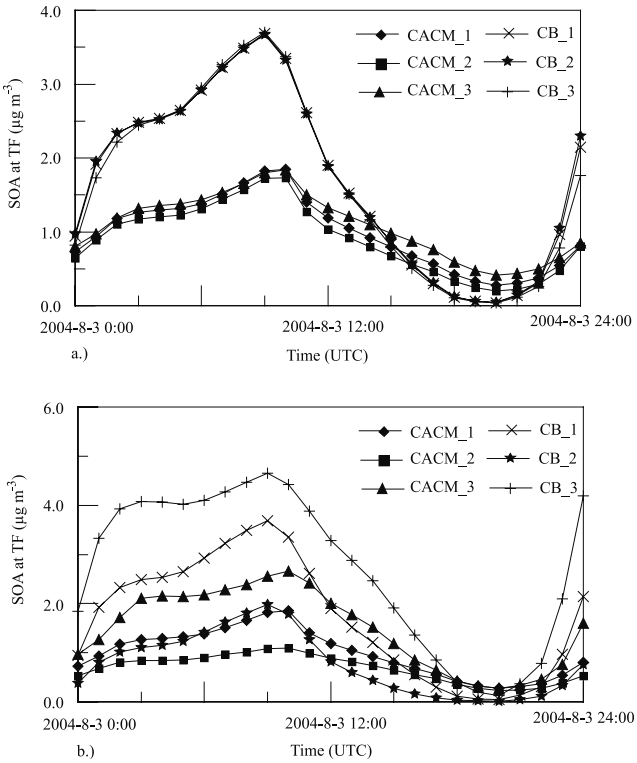

Figure 7. SOA predictions on 3 August 2004 at TF. (a) Domain-wide NO_x emissions were varied by ±40% from base case, and (b) temperature used in gas-phase chemistry and aerosol modules was varied by ±5 K from base case. Notation is as follows: _1 represents the base case, _2 represents the case with 40% increase of emissions for Figure 7a or the case with increase of temperature by 5K for Figure 7b, and _3 represents the case with 40% decrease of emissions for Figure 7a or the case with decrease of temperature by 5K for Figure 7b.

[34] On the contrary, an increase of NO_x emissions increases the oxidation power of the atmosphere at TF by leading to more O_3 and increased consumption of monoterpenes. This explains the very slight increase of SOA predicted by the simulation with CB-IV/SORGAM. Simulations with CACM/MPMPO and with CB-IV/SORGAM both predict higher SOA formation when domain-wide VOC emissions are increased, as would be expected.

[35] The sensitivity of SOA predictions to the temperature was conducted by adjusting by ±5 K the temperature that is fed into the gas-phase chemistry mechanism and the aerosol module. In this way, the temperature dependence of other processes such as emissions was not included. The dependence of SOA predictions on temperature (T) is stronger for CB-IV/SORGAM than for CACM/MPMPO. Twenty-four-hour average SOA prediction at TF in the (T − 5 K) case is 3.4 times that in the (T + 5 K) case for CB-IV/SORGAM, while for CACM/MPMPO, 24-hour average SOA prediction in the (T − 5 K) case is 2.1 times that in the (T + 5 K) case. The temperature dependence of SOA predictions is due mainly to the value used for enthalpy of vaporization of the SOA constituents. SORGAM uses 156.0 kJ mol^{-1} for all molecules, while MPMPO uses an average of approximately 73.0 kJ mol^{-1} depending on individual surrogate species. The values used in MPMPO are based on a molecular structure prediction technique [*Myrdal and Yalkowsky*, 1997]. Increases in the value of enthalpy of vaporization typically lead to greater predicted SOA [*Pun et al.*, 2003]. *Takekawa et al.* [2003] measured SOA yields from the photooxidation of toluene at different temperatures and found that the SOA yield at 283 K is approximately twice that at 303 K. Thus the temperature dependence predicted by both CACM/MPMPO and CB-IV/SORGAM is stronger than that measured experimentally. Temperature sensitivity in the eastern United States is similar to that observed for simulations in the SoCAB performed by *Vutukuru et al.* [2006].

4.3.2. Aqueous SOA

[36] A unique feature of the MPMPO module is that it simulates the simultaneous partitioning of semivolatile organics into both the organic and the aqueous phases, while other SOA modeling approaches typically only simulate the partitioning of semivolatile organics into one phase, usually organic. To evaluate the significance of partitioning of organics into the aqueous phase, the portion of SOA that resides in the aqueous phase was quantified. Figure 8 shows the predictions of 24-hour average aqueous-phase SOA from CACM/MPMPO for 3–4 August 2004. The maximum 24-hour average aqueous- phase SOA concentration is 0.43 μg m^{-3} for 3 August 2004, and 0.76 μg m^{-3} for 4 August 2004. However, these maxima are not spatially coincident with the maximum 24-hour average SOA concentration predictions from CACM/MPMPO shown in Figure 6. The aqueous-phase SOA can constitute from 0% to approximately 90% of the total SOA predictions from the MPMPO module. The relative importance of aqueous-phase SOA formation depends on multiple factors, among which are the LWC of aerosols, the aqueous-phase hydrogen ion concentration, and the competition with the partitioning to the organic phase. The MPMPO module does not treat potential further irreversible or reversible reactions (except ionization for carboxylic acids) for the organics in the aqueous phase despite observations of polymerization for certain compounds in the aqueous phase [*Hastings et al.*, 2005]. This suggests the current MPMPO module underestimates the importance of aqueous-phase SOA.

4.3.3. OM to OC Ratio

[37] Another strength of CACM/MPMPO is its ability to simulate organic composition. This enables calculation of the OM to OC ratio, which is used typically to convert measured aerosol OC content to aerosol OM [*Turpin and Lim*, 2001]. Figure 9 shows the spatial distributions of 24-hour average values for the average OM to OC ratio for the modeling domain. The average ratio varies from 1.10 to 1.90 in continental areas. In this study, the average OM to OC ratio is 1.16 for POA. The OM to OC ratio for surrogate species in the MPMPO module varies from 1.13 to 3.75, depending on the specific compound. The spatial distributions of average OM to OC show the spatial patterns of relative contributions of SOA and POA. In the northern part of the modeling domain, the average OM to OC ratio reaches 1.80 to 1.90 because of the dominant contributions of SOA to total OM. For areas where SOA formation is minor or where POA dominates over SOA formation, the average OM to OC ratio is in the range of

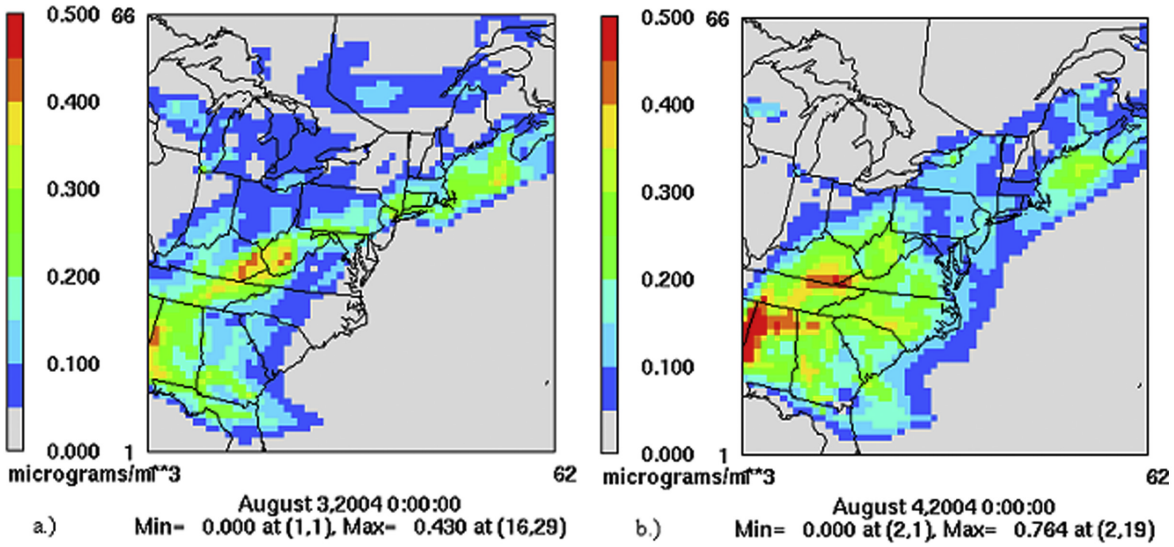

Figure 8. Predictions of 24-hour average aqueous-phase SOA from CACM/MPMPO: (a) 3 August 2004 (UTC) and (b) 4 August 2004 (UTC).

1.10 to 1.30. *Turpin and Lim* [2001] suggested that the average OM to OC ratio was 1.6 ± 0.2 for urban aerosols and 2.1 ± 0.2 for nonurban aerosols. The slightly lower OM to OC ratio from this study may be due to two reasons: a value of the OM to OC ratio used for POA that is too low and the potential under prediction of organic functionality for SOA from CACM/MPMPO.

5. Conclusions

[38] CACM and MPMPO have been incorporated into the CMAQ model and applied to the eastern United States for an August 2004 episode. Simulations with CACM/MPMPO were compared to simulations using CB-IV/SORGAM, as well as a number of observational data sets. Model simulations produce reasonable predictions for O_3, $PM_{2.5}$, sulfate, and ammonium but yield substantial underestimates for EC and OM. The underestimation of EC is probably due to the underestimation of emissions for EC. Reasons for the underestimation of OM may include uncertainties in the gas-phase mechanism and SOA modules used, the neglect of SOA formation from sesquiterpenes, isoprene, and additional formation pathways, and the potential underestimation of emissions of POA and parent hydrocarbons that are responsible for SOA formation.

[39] Simulations with CACM/MPMPO and with CB-IV/SORGAM produce similar SOA predictions for the nearly 40 sites where OM concentrations are available on 4 August 2004, based on 24-hour filter samples. Again, comparison to 24-hour filter samples is not the best method for dis-

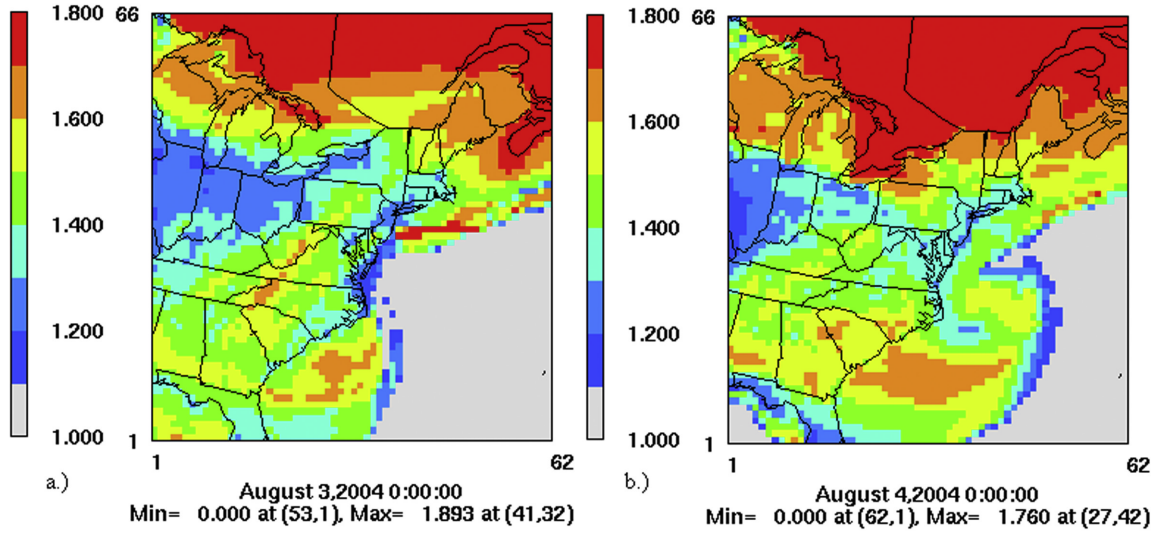

Figure 9. Spatial distributions for the 24-hour average values of the ratio of OM to OC from CACM/MPMPO: (a) 3 August 2004 and (b) 4 August 2004.

cussion of SOA model output discrepancies. However, responses of SOA predictions at TF to NO_x emissions changes and temperature variations are different for the two modeling approaches. This may lead to different results if both modeling approaches are used to examine the effect of NO_x emissions reductions on SOA concentrations or to study how climate change affects ambient SOA levels.

[40] **Acknowledgments.** Financial support for this work was provided in part by the Office of Oceanic and Atmospheric Research of NOAA under AIRMAP grants NA03OAR4600122 and NA04OAR4600154 and in part by the United States Environmental Protection Agency through STAR Research Assistance agreements R831083 and RD-83145401. Any opinions, findings, conclusions and/or recommendations expressed in this material are those of the authors and do not necessarily reflect the views of the funding agencies. We thank Gerry Gipson at EPA for providing the gas-phase chemical mechanism processor for the CMAQ model, Laura Cottrell and Luke Ziemba at the University of New Hampshire for providing the AMS data and particle filter data, Jennifer Hegarty and Tom Lambert at the University of New Hampshire for help with EPA AQS data, and Rodney Weber at the Georgia Institute of Technology for PILS data.

References

Aumont, B., S. Madronich, I. Bey, and G. S. Tyndall (2000), Contribution of secondary VOC to the composition of aqueous atmospheric particles: A modeling approach, *J. Atmos. Chem.*, *35*, 59–75.

Byun, D. W., and J. K. S. Ching (1999), Science algorithms of the EPA Models-3 Community Multi-scale Air Quality (CMAQ) modeling system, *Rep. EPA/600/R-99/030*, Off. of Res. and Dev., U. S. Environ. Prot. Agency, Washington, D. C.

Carter, W. P. L. (1990), A detailed mechanism for gas-phase atmospheric reactions of organic compounds, *Atmos. Environ., Part A*, *24*, 481–518.

Chen, J., and R. J. Griffin (2005), Modeling secondary organic aerosol formation from α-pinene, β-pinene, and d-limonene, *Atmos. Environ.*, *39*, 7731–7744.

Chow, J. C., J. G. Watson, E. M. Fujita, Z. Lu, D. R. Lawson, and L. L. Ashbaugh (1994), Temporal and spatial variations of $PM_{2.5}$ and PM_{10} aerosol in the Southern California Air Quality Study, *Atmos. Environ.*, *28*, 2061–2080.

deGouw, J. A., et al. (2005), The budget of organic carbon in a polluted atmosphere: Results from the New England Air Quality Study in 2002, *J. Geophys. Res.*, *110*, D16305, doi:10.1029/2004JD005623.

Ervens, B., G. Feingold, G. J. Frost, and S. M. Kreidenweis (2004), A modeling study of aqueous production of dicarboxylic acids: 1. Chemical pathways and speciated organic mass production, *J. Geophys. Res.*, *109*, D15205, doi:10.1029/2003JD004387.

Fredenslund, A., J. Gmehling, and P. Rasmussen (1977), *Vapor-Liquid Equilibrium Using UNIFAC*, Elsevier, New York.

Gery, M. W., G. Z. Whitten, J. P. Killus, and M. C. Dodge (1989), A photochemical kinetics mechanism for urban and regional scale computer modeling, *J. Geophys. Res.*, *94*, 12,925–12,956.

Griffin, R. J., D. R. Cocker III, R. C. Flagan, and J. H. Seinfeld (1999), Organic aerosol formation from the oxidation of biogenic hydrocarbons, *J. Geophys. Res.*, *104*, 3555–3567.

Griffin, R. J., D. Dabdub, M. J. Kleeman, M. P. Fraser, G. R. Cass, and J. H. Seinfeld (2002a), Secondary organic aerosol 3. Urban/regional scale model of size- and composition-resolved aerosols, *J. Geophys. Res.*, *107*(D17), 4334, doi:10.1029/2001JD000544.

Griffin, R. J., D. Dabdub, and J. H. Seinfeld (2002b), Secondary organic aerosol: 1. Atmospheric chemical mechanism for production of molecular constituents, *J. Geophys. Res.*, *107*(D17), 4332, doi:10.1029/2001JD000541.

Griffin, R. J., K. Nguyen, D. Dabdub, and J. H. Seinfeld (2003), A coupled hydrophobic-hydrophilic model for predicting secondary organic aerosol formation, *J. Atmos. Chem.*, *44*, 171–190.

Griffin, R. J., C. A. Johnson, R. W. Talbot, H. Mao, R. S. Russo, Y. Zhou, and B. C. Sive (2004), Quantification of ozone formation metrics at Thompson Farm during the New England Air Quality Study (NEAQS) 2002, *J. Geophys. Res.*, *109*, D24302, doi:10.1029/2004JD005344.

Griffin, R. J., D. Dabdub, and J. H. Seinfeld (2005), Development and initial evaluation of a dynamic species-resolved model for gas-phase chemistry and size-resolved gas/particle partitioning associated with secondary organic aerosol formation, *J. Geophys. Res.*, *110*, D05304, doi:10.1029/2004JD005219.

Guenther, A., C. Geron, T. Pierce, B. Lamb, P. Harley, and R. Fall (2000), Natural emissions of non-methane volatile organic compounds, carbon monoxide, and oxides of nitrogen from North America, *Atmos. Environ.*, *34*, 2205–2230.

Hansen, D. A., E. S. Edgerton, B. E. Hartsell, J. J. Jansen, N. Kandasamy, G. M. Hidy, and C. L. Blanchard (2003), The Southeastern Aerosol Research and Characterization Study: Part 1—Overview, *J. Air. Waste Manage. Assoc.*, *53*, 1460–1471.

Hastings, W. P., C. A. Koehler, E. L. Bailey, and D. O. DeHaan (2005), Secondary organic aerosol formation by glyoxal hydration and oligomer formation: Humidity effects and equilibrium shifts during analysis, *Environ. Sci. Technol.*, *39*, 8728–8735.

Heald, C. L., D. J. Jacob, R. J. Park, L. M. Russell, B. J. Huebert, J. H. Seinfeld, H. Liao, and R. J. Weber (2005), A large organic aerosol source in the free troposphere missing from current models, *Geophys. Res. Lett.*, *32*, L18809, doi:10.1029/2005GL023831.

Hoffmann, T., J. R. Odum, F. Bowman, D. Collins, D. Klockow, R. C. Flagan, and J. H. Seinfeld (1997), Formation of organic aerosols from the oxidation of biogenic hydrocarbons, *J. Atmos. Chem.*, *26*, 189–222.

Jang, M., N. M. Czoschke, S. Lee, and R. M. Kamens (2002), Heterogeneous atmospheric aerosol production by acid-catalyzed particle-phase reactions, *Science*, *298*, 814–817.

Jayne, J. T., D. C. Leard, X. Zhang, P. Davidovits, K. A. Smith, C. E. Kolb, and D. R. Worsnop (2000), Development of an Aerosol Mass Spectrometer for size and composition analysis of submicron particles, *Aerosol Sci. Technol.*, *33*, 49–70.

Jenkin, M. E. (2004), Modeling the formation and composition of secondary organic aerosol from α- and β-pinene ozonolysis using MCM v3, *Atmos. Chem. Phys.*, *4*, 1741–1757.

Jenkin, M. E., D. E. Shallcross, and J. N. Harvey (2000), Development and application of a possible mechanism for the generation of *cis*-pinic acid from the ozonolysis of α- and β-pinene, *Atmos. Environ.*, *34*, 2837–2850.

Jenkin, M. E., S. M. Saunders, V. Wagner, and M. J. Pilling (2003), Protocol for the development of the master chemical mechanism, MCMv3 (part B): Tropospheric degradation of aromatic volatile organic compounds, *Atmos. Chem. Phys.*, *3*, 181–193.

Johnson, D., S. R. Utembe, and M. E. Jenkin (2006), Simulating the detailed chemical composition of secondary organic aerosol formed on a regional scale during the TORCH 2003 campaign in the southern UK, *Atmos. Chem. Phys.*, *6*, 419–431.

Kalberer, M., et al. (2004), Identification of polymers as major components of atmospheric organic aerosols, *Science*, *303*, 1659–1662.

Kanakidou, M., et al. (2005), Organic aerosol and global climate modeling: A review, *Atmos. Chem. Phys.*, *5*, 1053–1123.

Kelly, N. A., and R. F. Gunst (1990), Response of ozone to changes in hydrocarbon and nitrogen oxide concentrations in outdoor smog chambers filled with Los Angeles air, *Atmos. Environ., Part A*, *24*, 2991–3005.

Kroll, J. H., N. L. Ng, S. M. Murphy, R. C. Flagan, and J. H. Seinfeld (2005a), Secondary organic aerosol formation from isoprene photooxidation under high-NO_x conditions, *Geophys. Res. Lett.*, *32*, L18808, doi:10.1029/2005GL023637.

Kroll, J. H., N. L. Ng, S. M. Murphy, V. Varutbangkul, R. C. Flagan, and J. H. Seinfeld (2005b), Chamber studies of secondary organic aerosol growth by reactive uptake of simple carbonyl compounds, *J. Geophys. Res.*, *110*, D23207, doi:10.1029/2005JD006004.

Lamb, B., D. Gay, and T. Pierce (1993), A biogenic hydrocarbon emission inventory for the U.S.A. using a simple forest canopy model, *Atmos. Environ., Part A*, *27*, 1673–1690.

Liggio, J., S. M. Li, and R. McLaren (2005), Reactive uptake of glyoxal by particulate matter, *J. Geophys. Res.*, *110*, D10304, doi:10.1029/2004JD005113.

Lim, H. J., A. G. Carlton, and B. J. Turpin (2005), Isoprene forms secondary organic aerosol through cloud processing: Model simulations, *Environ. Sci. Technol.*, *39*, 4441–4446.

Malm, W. C., J. F. Sisler, D. Huffman, R. A. Eldred, and T. A. Cahill (1994), Spatial and seasonal trends in particle concentration and optical extinction in the United States, *J. Geophys. Res.*, *99*, 1347–1370.

Mao, H., R. Talbot, D. Troop, R. Johnson, S. Businger, and A. M. Thompson (2006), Smart balloon observations over the North Atlantic: O_3 data analysis and modeling, *J. Geophys. Res.*, *111*, D23S56, doi:10.1029/2005JD006507.

McDonald, J. D., B. Zielinska, E. M. Fujita, H. C. Sagebiel, J. C. Chow, and J. G. Watson (2000), Fine particle and gaseous emission rates from residential wood combustion, *Environ. Sci. Technol.*, *34*, 2080–2091.

Myrdal, P. B., and S. H. Yalkowsky (1997), Estimating pure component vapor pressures of complex organic molecules, *Ind. Eng. Chem. Res.*, *36*, 2494–2499.

Nenes, A., S. N. Pandis, and C. Pilinis (1998), ISORROPIA: A new thermodynamic equilibrium model for multiphase multi-component inorganic aerosol, *Aq. Geochem.*, *4*, 123–152.

Pankow, J. F. (1994), An absorption model of the gas/aerosol partitioning involved in the formation of secondary organic aerosol, *Atmos. Environ.*, *28*, 189–193.

Presto, A. A., K. E. Huff Hartz, and N. M. Donahue (2005), Secondary organic aerosol production from terpene ozonolysis: 2. Effect of NO_x concentrations, *Environ. Sci. Technol.*, *39*, 7046–7054.

Pun, B. K., R. J. Griffin, C. Seigneur, and J. H. Seinfeld (2002), Secondary organic aerosol 2. Thermodynamic model for gas/particle partitioning of molecular constituents, *J. Geophys. Res.*, *107*(D17), 4333, doi:10.1029/2001JD000542.

Pun, B. K., S. Y. Wu, C. Seigneur, J. H. Seinfeld, R. J. Griffin, and S. N. Pandis (2003), Uncertainties in modeling secondary organic aerosols: Three-dimensional modeling studies in Nashville/western Tennessee, *Environ. Sci. Technol.*, *37*, 3647–3661.

Salcedo, D., et al. (2005), Characterization of ambient aerosols in Mexico City during the MCMA-2003 campaign with Aerosol Mass Spectrometry: Results from the CENICA supersite, *Atmos. Chem. Phys.*, *6*, 925–946.

Sandu, A., J. G. Verwer, J. G. Blom, E. J. Spee, G. R. Carmichael, and F. A. Potra (1997), Benchmarking stiff ODE solvers for atmospheric chemistry problems II: Rosenbrock methods, *Atmos. Environ.*, *31*, 3459–3472.

Saunders, S. M., M. E. Jenkin, R. G. Derwent, and M. J. Pilling (2003), Protocol for the development of the master chemical mechanism, MCMv3 (part A): Tropospheric degradation of non-aromatic volatile organic compounds, *Atmos. Chem. Phys.*, *3*, 161–180.

Saxena, P., and L. M. Hildemann (1996), Water-soluble organics in atmospheric particles: A critical review of the literature and application of thermodynamics to identify candidate compounds, *J. Atmos. Chem.*, *24*, 57–109.

Schell, B., I. J. Ackermann, H. Hass, F. S. Binkowski, and A. Ebel (2001), Modeling the formation of secondary organic aerosol within a comprehensive air quality model system, *J. Geophys. Res.*, *106*, 28,275–28,294.

Seigneur, C. (2001), Current status of air quality models for particulate matter, *J. Air Waste Manage. Assoc.*, *51*, 1508–1521.

Shah, S. D., D. R. Cocker III, J. W. Miller, and J. M. Norbeck (2004), Emission rates of particulate matter and elemental and organic carbon from in-use diesel engines, *Environ. Sci. Technol.*, *38*, 2544–2550.

Song, C., K. Na, and D. R. Cocker III (2005), Impact of the hydrocarbon to NO_x ratio on secondary organic aerosol formation, *Environ. Sci. Technol.*, *39*, 3143–3149.

Stockwell, W. R., P. Middleton, J. S. Chang, and X. Tang (1990), The second generation regional acid deposition model chemical mechanism for regional air quality modeling, *J. Geophys. Res.*, *95*, 16,343–16,367.

Sullivan, A. P., R. J. Weber, A. L. Clements, J. R. Turner, M. S. Bae, and J. J. Schauer (2004), A method for on-line measurement of water-soluble organic carbon in ambient aerosol particles: Results from an urban site, *Geophys. Res. Lett.*, *31*, L13105, doi:10.1029/2004GL019681.

Takekawa, H., H. Minoura, and S. Yamazaki (2003), Temperature dependence of secondary organic aerosol formation by photo-oxidation of hydrocarbons, *Atmos. Environ.*, *37*, 3413–3424.

Talbot, R., H. Mao, and B. Sive (2005), Diurnal characteristics of surface level O_3 and other important trace gases in New England, *J. Geophys. Res.*, *110*, D09307, doi:10.1029/2004JD005449.

Tanner, R. L., W. J. Parkhurst, M. L. Valente, and W. D. Philips (2004), Regional composition of $PM_{2.5}$ aerosols measured at urban, rural, and "background" sites in the Tennessee valley, *Atmos. Environ.*, *38*, 3143–3153.

Turpin, B. J., and H. J. Lim (2001), Species contributions to $PM_{2.5}$ mass concentrations: Revisiting common assumptions for estimating organic mass, *Aerosol Sci. Technol.*, *35*, 602–610.

Vizuete, W., V. Junquera, and D. T. Allen (2004), Sesquiterpene emissions and secondary organic aerosol formation potentials for southeast Texas, *Aerosol Sci. Technol.*, *38*, 167–181.

Vutukuru, S., R. J. Griffin, and D. Dabdub (2006), Simulation and analysis of secondary organic aerosol dynamics in the South Coast Air Basin of California, *J. Geophys. Res.*, *111*, D10S12, doi:10.1029/2005JD006139.

Zhang, Y., B. Pun, K. Vijayaraghavan, S.-Y. Wu, C. Seigneur, S. Pandis, M. Jacobson, A. Nenes, and J. H. Seinfeld (2004a), Development and application of the Model of Aerosol Dynamics, Reaction, Ionization, and Dissolution (MADRID), *J. Geophys. Res.*, *109*, D01202, doi:10.1029/2003JD003501.

Zhang, Y., B. Pun, S. Wu, K. Vijayaraghavan, and C. Seigneur (2004b), Application and evaluation of two air quality models for particulate matter for a southeastern U. S. episode, *J. Air Waste Manage. Assoc.*, *54*, 1478–1493.

J. Chen, R. J. Griffin, H. Mao, and R. W. Talbot, Institute for the Study of Earth, Oceans, and Space, University of New Hampshire, Durham, NH 03824, USA. (rjg@gust.sr.unh.edu)